Characterization of CDOM in saline and freshwater lakes across China using spectroscopic analysis

Kaishan Song†*[1]; Yingxin Shang†[1, 2]; Zhidan Wen[1]; Pierre-Andre Jacinthe[3], Ge Liu[1]; Lili Lyu[1]; Chong Fang[1, 2]

1. Northeast Institute of Geography and Agroecology, CAS, Changchun 130102, China

2. University of Chinese Academy of Sciences, Beijing 100049, China

3. Department of Earth Sciences, Indiana University-Purdue University Indianapolis, IN, USA

† K.S and Y.S contributed equally to this work.

* Corresponding author: Kaishan Song (songks@neigae.ac.cn)

Yingxin Shang (shangyingxin@neigae.ac.cn)

Zhidan Wen (wenzhidan@neigae.ac.cn)

Pierre-Andre Jacinthe (pjacinth@iupui.edu)

Ge Liu (liuge@neigae.ac.cn)

Lili Lyu (lvlili@neigae.ac.cn)

Chong Fang (fangchong@neigae.ac.cn)

Abstract: Colored dissolved organic matter (CDOM) is a major component of DOM in waters, and plays a vital role in carbon cycling in inland waters. In this study, the light absorption and three-dimensional excitation-emission matrix spectra (EEMs) of CDOM of 936 water samples collected in 2014–2017 from 234 lakes in five regions across

This is the author's manuscript of the article published in final edited form as:
Song, K., Shang, Y., Wen, Z., Jacinthe, P.-A., Liu, G., Lyu, L., & Fang, C. (2019). Characterization of CDOM in saline and freshwater lakes across China using spectroscopic analysis. Water Research, 150, 403–417. https://doi.org/10.1016/j.watres.2018.12.004

China were examined to determine relationships between lake water sources (fresh versus saline) and their fluorescence/absorption characteristics. Results indicated significant differences regarding DOC concentration and $a_{CDOM}(254)$ between freshwater (6.68 mg C L^{-1}, 19.55 m^{-1}) and saline lakes (27.4 mg C L^{-1}, 41.17 m^{-1}). While humic-like (F_5) and fulvic-like (F_3) compounds contributed to CDOM fluorescence in all lake waters significantly, their contribution to total fluorescence intensity (F_T) differed between saline and freshwater lakes. Significant negative relationships were also observed between lake altitude with either F_5 (R^2=0.63, N=306) or F_T (R^2=0.64, N=306), suggesting that the abundance of humic-like materials in CDOM tends to decrease with increased in lakes altitude. In high-altitude lakes, strong solar irradiance and UV exposure may have induced photo-oxidation reactions resulting in decreased abundance of humic-like substances and the formation of low molecular weight compounds. These findings have important implications regarding our understanding of C dynamics in lacustrine systems and the contribution of these ecosystems to the global C cycle.

Keywords: Absorption, CDOM, EEMs, freshwater, saline water

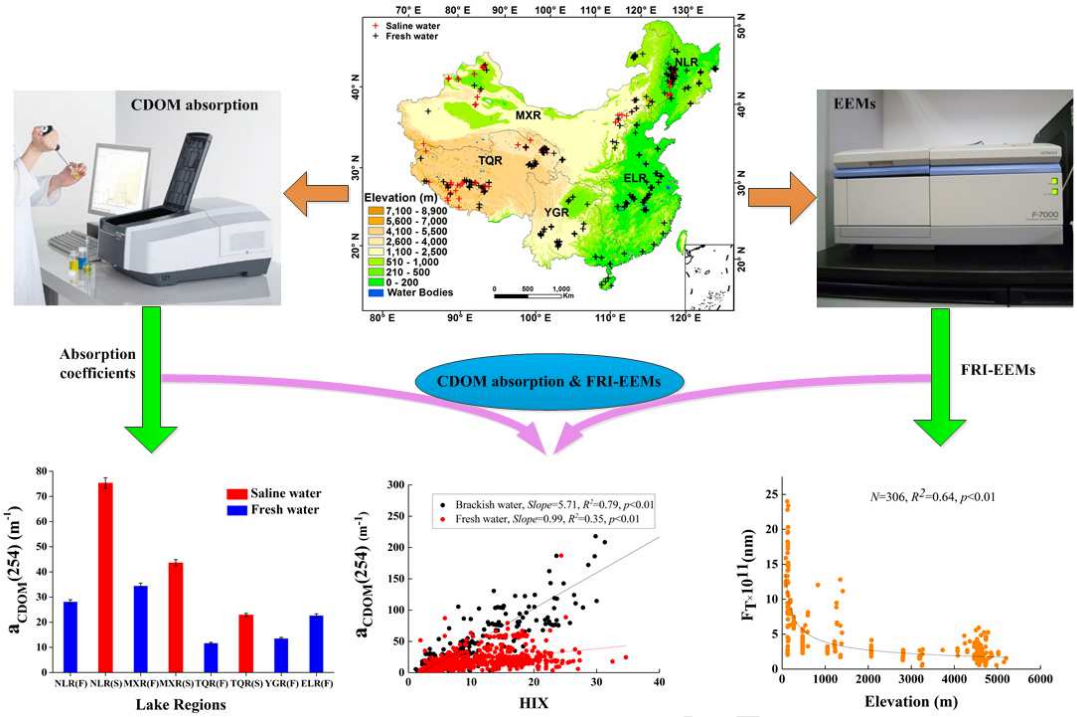

1. Introduction

Dissolved organic matter (DOM) is considered the largest pool of organic matter in natural waters, accounting for >90% of the total organic matter (Kececioglu et al., 1997; Cole et al., 2007; Para et al., 2010). Dissolved organic carbon (DOC) regulates metabolic and biogeochemical processes in water bodies, and ultimately determines the contribution of aquatic ecosystems to the global carbon cycle (Borge et al., 2015; Catalan et al., 2016). Part of the DOM is termed chromophoric dissolved organic matter (CDOM) based on the absorption of ultraviolet (UV) and photo-synthetically available radiation (PAR), whereas other DOM fractions are referred to as fluorescent DOM (FDOM) based on the emission of fluorescence photons after radiation absorption; both fractions are responsible for the optical properties of DOM (Effler et al., 2010). CDOM is a complex mixture of organic compounds of both allochthonous and autochthonous origin (Coble, 2007; Zhang et al., 2009). As an optically-active substance, CDOM absorption properties are significantly affected by several factors, including DOM concentration and its chemical composition (Minero et al., 2007), photo-induced and microbial processes in aquatic environments (Shank et al., 2010), and salinity (Singh et al., 2010).

Inland waters account for a significant portion of the global freshwater storage (Oki

& Kanae, 2006), and in China saline lakes comprise a large share of all inland waters (Ma et al., 2011). Although several studies and reviews have been carried out to examine the optical and chemical properties of CDOM, and evaluate relationships between salinity and CDOM fluorescence (Coble, 2007; Zhang et al., 2010; Moore et al., 2011; Song et al., 2013), little is known about the composition, sources, and the factors regulating the dynamics of CDOM in saline inland waters, especially across large national-scale regions. Previous studies have shown a linear inverse relationship between CDOM absorption and salinity (Singh et al., 2010), and elevated dissolved carbon concentration in inland waters from semi-arid and arid climates (Brooks and Lemon, 2007; Song et al., 2017). Increased water retention time in saline lakes could alter the absorption and fluorescence properties of CDOM through microbial degradation and strong photo-induced radiation reactions (Catalan et al., 2016). These phenomena are likely of lesser significance in freshwaters. Thus, studies are needed for characterizing CDOM absorption and fluorescence characteristics in inland saline waters (Duarte et al., 2008; Tranvik et al., 2009), and this is crucial to our ability to quantify the role of inland saline waters to the global carbon cycle (Cole et al., 2007; Tranvik et al., 2009). Moreover, the dynamics and characteristics of CDOM in saline waters may differ depending on their relative altitude (above sea level) and the amount

of solar radiation received. In high elevation saline lakes, exposure to UV-B radiation is expected to be significant and that could in turn increase the photo-chemical degradation of CDOM (Jansson et al., 2008). In addition, the terrestrial input of CDOM to aquatic systems is expected to be insignificant given the generally low terrestrial productivity and limited human activity in high altitude regions.

CDOM is a complex mixture of organic constituents, the composition of which is difficult to elucidate. Spectrophotometry and three-dimensional excitation-emission matrix spectra (EEMs) have provided useful information about CDOM composition, sources, and molecular size (Liu et al., 2007; Wang et al., 2007; Wen et al., 2018). Specifically, the spectral slope (S) provides important information on CDOM origin, chemical composition and sources (Fichot and Ronald, 2012), and the S value is a good proxy for indicating the proportion of terrestrial DOC in waters (Gonnelli et al., 2013). The $SUVA_{254}$ has been adopted to estimate the aromatic carbon content and to understand the chemical characteristics of DOM (Weishaar et al., 2003; Świetlik and Sikorska, 2004). In recent years, the EEMs fluorescence spectroscopy has been widely used to differentiate FDOM from fresh, riverine, coastal marine sources (Stedmon et al., 2003; Henderson et al., 2009; Zhao et al., 2016). Three popular methods have been used for extraction of useful information regarding FDOM, including the traditional

92 "peak-picking" method (Coble, 1996), EEM coupled with parallel factor analysis
93 (PARAFAC) (Stedmon et al., 2003), and EEM coupled with fluorescence regional
94 integration (FRI) (Chen et al., 2003; Yan et al., 2018). Compared to the PARAFAC
95 techniques, FRI is a quantitative approach that integrates all the wavelength-dependent
96 fluorescence intensity data and has been proven as an effective method to represent the
97 FDOM components. With the FRI method, five FDOM components (including
98 tyrosine-like component, tryptophan-like component, fulvic-like component, microbial
99 protein-like component, humic-like component) (Chen et al., 2003) have been identified,
100 and these components vary with the hydrologic conditions (such as water retention
101 time), geographical settings, climatic zones and regional landscape characteristics.
102 Therefore, FRI can be applied to large continental-scale examinations of CDOM
103 sources in different types of inland lakes (freshwater and saline) in an effort to identify
104 drivers of carbon cycling in these aquatic ecosystems.

105 In the present study, the FRI technique was used to identify the FDOM components
106 in 936 water samples from 234 lakes across five lake regions in China. The lakes
107 differed in salinity and elevation (relative to sea level, msl). We also determined the
108 absorption, source characteristics, and fluorescence of CDOM. The main objectives of
109 this study were to: (1) determine CDOM absorption coefficients in saline and freshwater

inland lakes; (2) characterize CDOM components with FRI and EEM techniques, and examine their potential for source tracking; (3) examine correlations between FRI-EEM parameters and CDOM absorption coefficients; and (4) examine the relationship between FDOM and elevation of saline lakes.

2 Materials and Methods

2.1 Five lake regions in China

Based on broad regional variations of landforms and climate characteristics, the lakes in China have been grouped into five regions (Ma et al., 2011), namely: Northeastern lake region (NLR), Inner Mongolia-Xinjiang lake region (MXR), Tibetan-Qinghai Plateau lake region (TQR), Yungui Plateau lake region (YGR) and Eastern lake region (ELR). The NLR is located in the humid and semi-humid monsoon climate zone, and the lakes (3.3% of all lakes in China) are mainly distributed in plain areas (Fig. 1). The formation of lakes is related to volcanic calderas, or to the formation of swamps on low-permeability geological formations. Due to the specific local geographical and climatic conditions, many saline soda lakes are formed in NLR (Song et al., 2013). The MXR lakes region is characterized by arid and semi-arid climate with low annual precipitation (175 mm) and high evaporation level. Many lakes in the MXR region are

brackish to salty. The TQR is located in an area with an average elevation over 4,000 m (above msl). The high altitude and strong solar radiation contribute to the unique ecological characteristics of that region. Largely associated with endorheic drainage basins, most of the TQR lakes are saline. The TQR region includes some of the highest alpine lakes on the Earth, and represents an area with the highest density of lakes in the world. The YGR is located in a subtropical monsoon climate zone. The lakes in this region are formed along fault zone or steep valleys, and are mostly tectonic lakes. The ELR region, situated in the middle/lower reaches of the Yangtze River, Yellow River, Hai River and Huai River, is the most developed region in China. About 30% of the total lake areas in China are centered in the ELR, including the largest five freshwater lakes in the country (Fig. 1).

[Insert Fig.1 about here]

2.2 Field sampling and measurements

Both freshwater lakes and saline water lakes (Electrical conductivity (EC) threshold: 1,000 μS cm^{-1}) were selected in the five lake regions across China in order to characterize the features of FDOM among freshwater or saline water lakes. Lakes were selected with respect to both salinity and watershed characteristics. In total, 936 water samples (630 freshwater, 306 saline) were collected from 234 lakes between 2014 and

2017. For each sampling point, geographical coordinates (latitude, longitude) and elevation were recorded *in situ* with a GPS receiver. Some water chemical parameters including EC, turbidity, temperature were measured in situ with an YSI EXO1 portable multi-parameter water quality probes. At the time of sampling, water clarity was also determined with a Secchi disk depth (SDD). All lake water samples were collected in 1-L acid-cleaned plastic bottles, held on ice packs, and transported to the laboratory as soon as possible. In the laboratory, samples were stored at 4℃ in a refrigerator, and analyzed within 2 days.

2.3 Water quality measurements

In the laboratory, water samples were analyzed for DOC concentration on a Shimadzu TOC-5000 Analyzer (680 ℃). Total nitrogen (TN) and total phosphorus (TP) were analyzed according to APHA/AWWA/WEF (1998). Chlorophyll-a concentration was obtained through extraction of a filtered sample (0.45 μm Whatman GF/F) with 90% acetone solution, and determination of the chlorophyll-a concentration (*Chl-a*) with a Shimazdu UV-2600PC spectrophotometer. Total suspended matter (TSM) was obtained gravimetrically as described in Song et al. (2013).

2.4 CDOM absorption analysis

The water samples in the laboratory were filtered through a 0.7 µm pre-combusted Whatman GF/F filter, and then through a 0.22 µm Millipore membrane cellulose filter. CDOM absorption spectra were determined using a Shimadzu UV-2600PC UV–Vis spectrophotometer, fitted with a 1-cm quartz cuvette, in the spectral region between 200 and 800 nm at 1 nm intervals. CDOM spectra for Milli-Q water was used as reference. The CDOM absorption coefficient ($a_{(\lambda)}$) was computed according to Eq.1:

$$a_{(\lambda)} = 2.303A_{(\lambda)} / L \quad (1)$$

where L is the cuvette length (m), and $A_{(\lambda)}$ the measured optical density.

The spectral absorbance can be modeled with Eq. 2:

$$a_{CDOM}(\lambda)=a_{CDOM}(\lambda_0)\exp(-S^{(\lambda-\lambda 0)}) \quad (2)$$

where λ_0 is a reference wavelength of 700 nm and S is the spectral slope.

In this study, the absorption coefficient of CDOM at 254 nm (a_{254}) was used as a proxy for CDOM concentration. The spectral slope (S) between 275-295 nm ($S_{275-295}$) was calculated using Eq. 2, and used as a proxy for DOM molecular weight which is linked to CDOM sources (Helms et al., 2008; Zhang et al., 2011). The specific UV absorbance at 254 nm ($SUVA_{254}$) is defined as the absorbance at 254 nm (m^{-1}) divided by the DOC concentration (mg C L^{-1}) (Weishaar et al., 2003). Unlike $S_{275-295}$, $SUVA_{254}$

increases with decreasing CDOM molecular size (Song et al., 2017).

2.5 CDOM fluorescence measurement and FRI analysis

CDOM fluorescence excitation-emission matrices (EEMs) were measured using a Hitachi F-7000 fluorescence spectrometer equipped with a 700-V xenon lamp. The excitation (Ex) and emission (Em) scanning ranges were 200-450 nm (5 nm intervals) and 250-500 nm (1 nm intervals), respectively. The spectra were recorded at a scan rate of 2400 nm min^{-1} using excitation and emission slit bandwidths of 5 nm. EEMs of Milli-Q water blanks were subtracted to eliminate the water Raman scatter. The elimination of the inner-filter effect was performed by adjusting for CDOM absorbance at the corresponding wavelengths according to Eq. 3 (McKnight et al., 2001; Kothawala et al., 2013). Interpolation was used to remove the effect of Rayleigh scattering (Stedmon and Bro, 2008).

$$F_{cor}=F_{obs}\times 10^{(A_{Ex}+A_{Em})/2} \quad (3)$$

where F_{obs} and F_{cor} represent fluorescence intensity of EEMs before and after calibration, respectively. The A_{Ex} and A_{Em} represent corrected absorbance at the corresponding excitation and emission wavelengths, respectively. The fluorescence was normalized to the integral of Raman signal to eliminate the effect daily variation in lamp intensity (Lawaetz and Stedmon, 2009).

[Insert Table 1 about here]

Fluorescence regional integration (FRI) is a new quantitative approach to analyze the total wavelength-independent fluorescence intensity data based on EEM spectra (Chen et al., 2003; Sun et al., 2016). EEM maps were divided into five regions, and a description of each region is provided in Table 1. The integral volume (F_i) can be expressed as follows:

$$F_i = \sum_{Ex}\sum_{Em} I(\lambda_{Ex}\lambda_{Em})\,\Delta\lambda_{Ex}\Delta\lambda_{Em} \quad (4)$$

where $I(\lambda_{Ex}\lambda_{Em})$ is the fluorescence intensity at each excitation–emission wavelength pair. $\Delta\lambda_{Ex}$ is the internal excitation wavelength (taken as 5 nm), $\Delta\lambda_{Em}$ is the internal emission wavelength (taken as 5 nm). The sum of the fluorescence intensities of FRI-divided FDOM components were presented by F_T (unit: nm). The percent fluorescence response in a specific region (P_i = 1, 2, 3, 4, 5) was calculated as following:

$$P_i = {}^{F_i}/_{F_T} \times 100\% \quad (5)$$

The humification index (HIX) represents the ratio of allochthonous fluorescence intensity $F_{3\&5}$ to that of the autochthonous fluorescence intensity $F_{1\&2\&4}$ (Bilal et al., 2010). Humic-like fluorescence indicated as $F_n(355)$ was excited at 355 nm and its emission was measured at 445-455nm (Vignudelli et al., 2004).

2.6 Statistical analyses

Statistical analyses, including mean values, standard deviations, linear or non-linear regressions, and t-tests were performed using SPSS 16.0 software package (Statistical Program for Social Sciences, Chicago, IL). Difference is considered statistically significant when $p < 0.05$. Spatial mapping of sampling sites and land cover types were conducted using ArcGIS 10.1 (Environmental Systems Research Institute, Redlands, CA). Principal components analysis (PCA) was conducted using Origin 9.0 (Microcal Software, Inc., Northampton, MA) by using the five FRI fluorescent components according to different trophic status and lake regions.

3. Results

3.1 Biogeochemical characteristics

Analysis results of the 936 lake water samples collected in the present study indicated that the lakes studied in the five lake regions of China are diverse, not only in terms of their geomorphological and climatic settings, but also in regards to water chemistry as exemplified by the difference in DOC, TN, TP, *Chl-a*, TSM and EC values for lakes in the different regions (Table 2). The differences in water quality parameters among lakes from the five regions were all statistically significant ($p<0.001$).

The average DOC and TN, TP concentration in the saline waters was noticeably

higher than that of the freshwater lakes (Table 2). The difference in DOC concentration (and other water chemical parameters) between saline water and freshwater lakes was statistically significant ($p<0.001$). Among the five lake regions of China, DOC concentration ranged from 5.25 to 35 mg C L^{-1} (Fig.2a), with a mean DOC concentration of 27.4 and 6.68 mg C L^{-1} for saline and freshwater lakes, respectively. The DOC concentration in NLR, MXR and TQR region lakes were higher than that of lakes from the ELR and YGR regions. The mean TN concentration in the five lake regions was, from highest to lowest, in the order: NLR (5.54 mg N L^{-1}), TQR (3.82 mg N L^{-1}), MXR (3.23 mg N L^{-1}), ELR (0.98 mg N L^{-1}) and YGR (0.90 mg N L^{-1}). Similarly, the TP concentration exhibited significant regional variability, ranging from 0.02 to 1.28 mg P L^{-1}. The highest TN and TP were measured in the NLR lakes, and the lowest TN was observed in lakes from the YGR region, while the lowest TP concentration was observed in the ELR region lakes. The EC values and TSM concentration in the saline lakes was higher than in the freshwater lakes. The mean EC of lake waters ranged from 345.3 to 12,722.9 µS cm^{-1}. The range for *Chl-a* concentration was 1.94 to 55.21 µg L^{-1} for different regions. The highest EC (12,722.98 µS cm^{-1}) was observed in the TQR while the highest *Chl-a* concentration was found in the ELR (55.21 µg L^{-1}). All of the water chemical parameters in saline waters were

253 significantly different for each lake region ($p<0.01$).

254 **[Insert Table 2 about here]**

255 **[Insert Fig. 2 about here]**

256 **3.2 CDOM absorption characteristics**

257 Among the 936 lake water samples, $a_{CDOM}(254)$ ranged from 1.39 m^{-1} to 530.03 m^{-1},
258 with a mean of 41.17 m^{-1} for saline lakes and 19.55 m^{-1} for freshwater lakes. The
259 $a_{CDOM}(254)$ of saline lakes were significantly different from that of fresh lakes ($p<0.01$).
260 When all five lake regions were considered together, the $a_{CDOM}(254)$ in saline waters
261 were much higher than that of the freshwaters in the NLR, MXR and TQR (Fig.2b).
262 Another interesting result of this study (Fig.2b) is that, for the saline lakes in the NLR,
263 MXR and TQR region, the CDOM absorption at 254 nm decreased significantly with
264 increased lakes elevation.

265 The $S_{275-295}$ in this study ranged from 10 μm^{-1} to 61.15 μm^{-1}, and the mean values
266 were 0.031nm^{-1} for saline lakes and 0.024 nm^{-1} for freshwater lakes (Fig.3a). The slope
267 for both saline lakes and freshwater lakes in the five regions were significantly different
268 ($p<0.01$). The CDOM slopes for saline lakes in each individual lake region were higher
269 than that of the freshwater lakes in that region. The $S_{275-295}$ increased while the $SUVA_{254}$
270 decreased inversely. The $SUVA_{254}$ in this study ranged from 0.04 to 5.62 L $mg^{-1}m^{-1}$ for

saline waters, and from 0.35 to 6.99 L $mg^{-1}m^{-1}$ for freshwaters (Fig.3b). The $SUVA_{254}$ for both saline and freshwater lakes in the five regions were significantly different ($p<0.01$). The $SUVA_{254}$ for saline lakes in a given region was significantly lower than that of freshwater lakes in the corresponding region. For both freshwater and saline lakes, we observed a significant ($p<0.01$) increase in the $S_{275-295}$ values with increased lakes elevation in the NLR, MXR and TQR regions. In contrast, a corresponding decrease in $SUVA_{254}$ values with increased lakes elevation was noted. We had also organized our dataset with seasons (spring, summer and autumn), it was found that $S_{275-295}$ of saline waters in all three seasons was higher than that of fresh waters, the inverse trends of $SUVA_{254}$ was also observed in the corresponding seasons (Fig. S3a-b). For all water types and seasons, the $a_{CDOM}(254)$, $SUVA_{254}$ were all negatively correlated to elevation ($p<0.01$) (Table S1). Details of these intriguing phenomena will be discussed in later sections.

[Insert Fig. 3 about here]

3.3 FRI-Based CDOM Fluorescent Components

In this study, the FRI-based EEMs in saline and freshwater lakes of China were analyzed to document trends in CDOM fluorescence characteristics in relation to lake types. The excitation-emission area volumes F_i and P_i (i = 1, 2, 3, 4, and 5) were

289 proportional to the total fluorescence intensity and the relative contribution of the five
290 different components to the total fluorescence intensity. Examples of EEM fluorescence
291 spectra from Lake Seli Co (TQR), Lake Aibi (MXR) and Lake Khanka (NLR) were
292 selected as representative of lakes in these regions (Fig. 4). The total fluorescence
293 intensity (F_T) ranged from 3.78×10^{10} nm to 4.55×10^{12} nm for all water samples, and
294 the mean F_T for saline waters and freshwaters was 4.91×10^{11} nm and 3.39×10^{11} nm
295 respectively (Fig. 5). The F_T in saline waters was higher than that of the freshwaters in
296 lakes from the NLR, MXR and TQR. The highest F_T (1.05×10^{12} nm) was observed in
297 the saline waters from the NLR, while the lowest F_T (1.99×10^{11} nm) was obtained in
298 the freshwaters from the TQR. For different seasons, the corresponding FRI-EEM
299 component in the fresh waters was lower than that of saline waters for various seasons
300 (Fig. S3c-d).

301 The relative contribution of individual components (F_i, with i=1, 2, 3, 4, 5) to total
302 fluorescence intensity differed among lake types and regions (Fig. 6). It was found that,
303 for both saline and freshwater lakes in different regions, the F_5 (humic-like) and F_3
304 (fulvic-like) compounds were predominant in FDOM. Furthermore, by comparing the
305 fluorescence intensity of different components (P_i, with i= 1, 2, 3, 4, 5) across lake
306 regions (Fig.7), it was found that the percent of F_5 to total fluorescence intensity in

307 saline lakes was higher than that of freshwater lakes in the NLR, MXR and TQR
308 regions. The inverse was observed in regard to the F_3 fluorescent component. These
309 results indicated that the fluorescence intensity of the five components and their relative
310 contribution to the total fluorescence intensity differed between saline and freshwater
311 lakes across the five lake regions of China. The Fn(355) ranged from 3.28 to 1,018 nm,
312 with a mean Fn(355) of 108.50 and 88.75 nm for freshwater and saline lakes,
313 respectively. The relative humic-like fluorescence content of saline waters was higher
314 than that of the freshwaters. However, the mean humification index (HIX) for
315 freshwater lakes (8.45) was nearly 2-fold higher than for saline waters (4.39).

316 **[Insert Fig. 4-7 about here]**

317 **3.4 PCA of FRI Fluorescent Components**

318 PCA was conducted, using the relative scores of the five FRI fluorescent components
319 (F1, F2, F3, F4 and F5) for all 936 lake water samples, to determine the degree of
320 separation between the saline lakes and freshwater lakes investigated. For the saline
321 lakes, the first two PCA axes (i.e., components 1 and 2) explained 91.2% of the total
322 variance in the dataset, with component 1 and component 2 accounting for 68.1% and
323 23.1%, respectively (Fig.8a). For the freshwater lakes, the first two PCA axes (i.e.,
324 components 1 and 2) explained 96.4% of the total variance in the dataset, with

component 1 and component 2 accounting for 82.5% and 14.9%, respectively (Fig. 8c). Each PCA axis is a linear combination of the five FRI fluorescent components (Table 3).

[Insert Fig.8 and Table 3 about here]

The five FRI fluorescent components showed positive component 1 loadings (Fig. 8a and 8c). The fulvic-like (F_3) and humic-like (F_5) compounds showed positive loadings for component 2. The FRI-PCA in this study could differentiate, on the basis of fluorescent characteristics, between the allochthonous substances [fulvic-like (F_3) and humic-like (F_5) compounds] and the autochthonous substances [tyrosine-like (F_1), tryptophan-like (F_2), and microbial protein-like (F_4) compounds]. Further, a plot of the PCA component 1 and component 2 scores for all 306 saline water samples (Fig. 8b) showed a general clustering of most saline water samples, with component 1 scores in the range of -3 to 8 and component 2 scores ranging from -3 to 4. The water samples from the NLR region lakes were generally scattered, with high component 1 and component 2 scores. However, the saline water samples from TQR lakes were generally clustered along the negative axis of component 1 and component 2. With increased in altitude from NLR and MXR to the TQR region lakes, the PCA score distribution for the saline samples decreased along the vertical axis of component 2. In contrast, for the

343 freshwater lake samples (scores ranging from -2 to 4 for PCA component 1 and from -1
344 to 3 for PCA component 2), the scores distribution (Fig. 8d) was random and did not
345 follow patterns that could be associated with specific lake regions (although a weak
346 cluster was noted for samples from YGR and TQR along the negative axis of
347 component 2).

348 **[Insert Fig. 8 about here]**

349 # 4. Discussion

350 ## 4.1 DOC and CDOM absorption of saline and freshwaters

351 Variability in DOC concentration among the inland lakes investigated reflects the
352 diversity of the geological materials, land use, climatic conditions and human activity
353 within the lakes drainage basins (Tranvik et al., 2009; Webster et al. 2008). The range of
354 DOC concentration (5.25-35.07 mg C L^{-1}; Fig. 2a) measured in the present study
355 overlaps nicely the results of an earlier study by Song et al. (2013) in which DOC
356 concentration in the range of 3.61-32.60 and 1.01-14.23 mg C L^{-1} was measured in
357 saline and freshwater lakes, respectively. Similar results have also been reported by
358 Curtis and Adams (1995) for lakes in the semi-arid region of Alberta, Canada. The high
359 DOC content in saline water indicated that DOC tends to accumulate with long water
360 retention time (Catalan et al., 2016), and may also reflect the input of carbonaceous

materials transported via runoff from surrounding landscapes (Spencer et al., 2012; Song et al., 2013).

A key finding of the present study is the observation that, in both freshwater and saline lakes, DOC concentration tends to decrease gradually with increased lakes altitude in the NLR and MXR to the TQR region. Conversely, in YGR and ELR regions, DOC concentration tends to rise consistently with decreased lake elevation. A similar trend was previously reported in the YGR region by Zhang et al. (2009). Indeed, different land use types (Fig. S1) and climatic conditions may have contributed to the variability in DOC input and DOC optical characteristics. For example, the much higher DOC concentration and predominance of humic substances in lake waters from the NLR region could be ascribed to the forestland and unique soils in that region (Zhao et al., 2016). But above all, our research findings revealed that landscape elevation plays an important role in driving the DOC variability.

The $a_{CDOM}(254)$ for saline waters was significantly different ($p<0.01$) from that of freshwaters across the five regions (Fig. 2b). Compared with other previous studies, our $a_{CDOM}(254)$ values were comparable to the results of Zhang et al. (2018) who reported $a_{CDOM}(254)$ between 1.68 and 92.65 m^{-1} for 22 lakes along a trophic gradient in China. The diversity of CDOM absorption at 254 nm may be due to the following factors.

Firstly, the CDOM absorption is dependent on the total DOM concentration in the lake waters. The regional hydrogeological conditions and the variety of climatic situations additionally affect the variability of DOM in lake waters. Because of the prevailing dry climate in the areas surrounding most of the saline lakes, high rates of evaporation likely occur and that may have contributed to the high DOM concentrations measured in these lakes. Secondly, the saline waters are generally terminal lakes in semi-arid or arid regions, and consequently DOM from terrestrial sources accumulates in these lakes (and is not exported downstream).

4.2 CDOM sources for saline and freshwaters

The slopes for both saline lakes and freshwater lakes in the five regions were significantly different ($p<0.01$). The CDOM slopes for saline lakes in the five regions were all lower than those of the freshwater lakes in the corresponding regions (Fig. 3a). This observation is similar to those of Wen et al. (2016) who noted that the slope of CDOM absorption for Mongolian plateau saline lakes dominated by autochthonous sources of CDOM was higher than that of freshwater rivers in the region. In contrast, in many fresh water lakes, significant input of CDOM from surrounding landscapes can occur, especially during extreme hydrological events. This interpretation is in line with the work of Zhou et al. (2016) who reported a parallel increase in the concentration and

397 relative molecular size of terrestrial humic-like CDOM molecules in Qiaodao Lake
398 waters during periods of high inflow.

399 In the saline lakes across different regions, we observed a significant increase in
400 $S_{275-295}$ with increase in the altitude of the lakes, from NLR and MXR to TQR region,
401 while the $SUVA_{254}$ values significantly decreased (Fig. 3b). Our $SUVA_{254}$ results
402 (Fig.3b) were similar to those reported for terminal lakes of the Innner Mongolia
403 Plateau (saline waters, $SUVA_{254}$=1.90 mg C^{-1} m^{-1}; freshwaters, $SUVA_{254}$=2.74 mg C^{-1}
404 m^{-1}), and for saline lakes of Northeast China (2.8-5.7 mg C^{-1} m^{-1}) (Wen et al., 2016;
405 Zhao et al., 2017). The higher S and lower $SUVA_{254}$ may be due to the effect of salinity
406 on photosynthesis in terrestrial higher plants, and to microbial degradation and the
407 stronger photo-degradation processes resulting from prolonged water residence time and
408 greater UV radiation exposure.Wu et al., 2005; Brooks et al., 2007; Madsen-Østerbye et
409 al., 2018). Moreover, our results suggest that the proportion of terrigenous DOC in
410 saline waters was lower than that of the freshwater lakes. The diversity of
411 hydrogeological conditions, longer residence time of DOM and the photo-degradation
412 of DOM in saline waters could significantly contribute to the variability of CDOM
413 absorption and composition (Spencer et al., 2012; Song et al, 2013; Wen et al., 2018).
414 This result was consistent with Kellerman et al. (2015) who concluded that degradation

processes preferentially remove oxidized, aromatic compounds in aquatic systems.

[Insert Fig.9 about here]

The differences in the correlation between DOC and CDOM for saline waters and freshwaters suggest that salinity may have modulated the relationships between these variables in the lakes investigated. Our results were similar to those from previous studies that have reported good correlations between CDOM absorption and DOC in coastal areas and inland waters (Chen et al., 2002; Rochelle-Newall and Fisher, 2002; Song et al., 2018). But, the variability in the strength of these correlations for different regions was ascribed to differences in regional geological characteristics and salinity. The presence of CDOM components such as allochthonous fulvic and humic acids can also be responsible for the good correlation that is usually observed between CDOM absorbance and DOM content in a variety of waters (Vione et al., 2010). Therefore, the results indicated that human disturbances, non-point agricultural pollutant and climatic conditions may have contributed to the accumulation of terrestrial humic acids in the freshwater lakes investigated. The general slope gradient was in the order (from high to low): TQR, MXR and NLR. The high slopes DOC/CDOM (Fig.9) indicate that the higher slopes in saline lakes were associated with the high autochthonous production CDOM and photo-induced degradation of CDOM. The photo-chemical degradation of

CDOM changed its optical and chemical properties; it involves the decomposition of CDOM chromophores and results in reduced CDOM absorptivity of UV and visible radiations (Fichot and Miller, 2010). Finally, due to long water retention time of saline lakes, more aromatic compounds for allochthonous matters are preferred to degradation to form low molecular CDOM components that may have also influenced CDOM composition and ultimately the correlation between CDOM and DOC.

4.3 Correlation between CDOM and Fluorescent Components

The PCA results for saline waters indicated that the fulvic-like (F_3) and humic-like (F_5) components were predominant in FDOM for saline waters in the NLR region. With increased lake altitude, the contribution of autochthonous substances increases in saline waters. The PCA score of the freshwaters indicated that the fluorescent CDOM varied with different hydrogeological conditions within individual lake regions, and that the allochthonous substances (F_3 and F_5) were predominant in the terminal lakes of NLR and MXR regions while the more autochthonous substances (F_1, F_2 and F_4) were produced in lakes of the YGR and TQR regions. Conversely, the high percentage of F_1, F_2 and F_4 in the ELR lakes indicated that the low-altitude freshwater lakes in that region are highly polluted, exhibiting high content of the tyrosine-like, tryptophan-like, and

451 microbial protein-like materials. This interpretation is consistent with previous studies
452 (Baker, 2001; Lu et al., 2014; Zhao et al., 2017). Baker (2001) related the high
453 fluorescence intensity of the tryptophan-like component of FDOM to wastewater
454 discharge. Likewise, Zhao et al. (2017) detected the highest concentration of the
455 tryptophan-like and the microbial protein-like components in highly polluted river
456 basins. Lu et al. (2014) concluded that anthropogenic activities (cropland, pasture and
457 urban) increased microbial activity and enhanced the relative abundance of protein-like
458 fluorescence of DOM.

459 **[Insert Fig. 10 about here]**

460 Correlations among the five fluorescent components and with other optical
461 parameters [$a_{CDOM}(254)$, HIX and Fn(355)] showed, for both saline and freshwater lakes,
462 strong positive linear relationships between F_1 and F_4 (Fig.10a) (saline waters: R^2=0.71,
463 $p<0.01$; freshwaters: R^2=0.93, $p<0.01$), suggesting that parts of the tyrosine-like
464 component F_1 and microbial protein-like component F_4 are likely from the same
465 autochthonous sources. Similar results were also found between F_3 and F_5 (Fig.10b)
466 which indicated that the fulvic-like components F_3 and the humic-like components F_5
467 may originate from similar allochthonous sources. The saline lakes are largely
468 distributed in the endorheic region of China, and are characterized by long water

residence times and strong water evaporation. Consequently, organic materials (autochthonous and allochthonous) progressively accumulate in these lakes along with salinity, and that may have contributed to the greater concentration of CDOM and FDOM measured in the saline lakes (Catalan et al., 2016; Song et al., 2018). Strong positive correlations between the tryptophan-like F_2 and the fulvic-like components F_3 were observed in saline waters (Fig.10c) (slope=0.03, R^2=0.67) and in freshwater lakes (slope=0.09, R^2=0.54), indicating that part of the tryptophan-like fluorophore may have originated from the fulvic-like components, and that the ratio of tryptophan-like component to fulvic-like component was higher in freshwaters than in saline waters. There was also a weak correlation between the total allochthonous substance $F_{3\&5}$ and the $a_{CDOM}(254)$ for saline waters (slope=0.07, R^2 =0.39) and freshwaters (slope=0.03, R^2=0.39) (Fig.10d). Moreover, correlation between $a_{CDOM}(254)$ and Fn(355) were also found for saline waters (slope=0.27, R^2 =0.54) and freshwaters (slope=0.18, R^2 =0.61) individually. These results suggested that the CDOM was dominated with allochthonous substances in both saline waters and freshwaters. There were also moderate positive linear relationships between $a_{CDOM}(254)$ and HIX for saline waters (slope=5.71, R^2 =0.79) and freshwaters (slope=0.99, R^2 =0.35) respectively. These results indicated that the relative humic-like components were more abundant in freshwaters, in accord with

higher degree of humification of CDOM in freshwater than in saline waters. Long periods of exposure to sunlight have likely increased the extent of photochemical oxidation processes in saline waters. The photo-production process significantly increases with salinity in natural waters (Nieto-Cid et al., 2006; Mostofa et al., 2009; Osburn et al. 2009). Our result indicated that the linkage of the fluorescent CDOM components to CDOM in saline waters and freshwaters can be very complex due to the effect of various hydro-geographical and climatic factors, including precipitation, salinity, wastewater discharge and the trophic status of the lakes.

4.4 Elevation versus FDOM components for saline water

Examination of the correlations between lake elevation and fluorescent CDOM characteristics showed weak relationships between these variables in the freshwater lakes (Fig. S2). However, as shown in the results, for all water types (fresh waters and saline waters) and seasons, the $a_{CDOM}(254)$, $SUVA_{254}$, F_5 and F_T were all negatively correlated to elevation ($p<0.01$) (Table S1). This result indicated that with the increasing of elevation, less human activity decreased CDOM input, and stronger photochemical degradation of allochthonous CDOM, and seasonal changes and elevations would affect the CDOM compositional changes in fresh waters mutually significantly. Therefore, the sole effect of elevation on fluorescent characteristics of CDOM was not as pronounced

505 as in saline waters. Future studies could investigate the seasonality of CDOM
506 composition in lakes of different altitudes especially for fresh waters. Meanwhile, these
507 relationships are likely driven by variations in geological settings, climate
508 characteristics, irradiance conditions, and anthropogenic factors and their effect on
509 water residence time and DOC dynamics in lacustrine systems. The short water
510 retention time as well as differences in the origin of CDOM may account for the weak
511 relationships observed in the freshwater lakes (Moran et al., 2000; Winter et al., 2007;
512 Catalan et al., 2016).

513 **[Insert Fig.11 about here]**

514 The correlation between elevation and CDOM absorption at 254nm (R^2=0.51,
515 N=306), and between elevation and $SUVA_{254}$ in the saline lakes (R^2=0.41, N=306) was
516 moderate (Fig. 11a and 11f). These trends indicated that the CDOM absorption was
517 higher in the high altitude than in the lower altitude lakes, and that the molecular weight
518 and aromaticity of CDOM trends to decrease with increased lakes elevation. No strong
519 correlations between the tyrosine-like F_1, the tryptophan-like F_2, and the microbial
520 protein-like F_4 components were observed. There was a negative linear correlation
521 between the humic-like F_5 and elevation (R^2=0.63, N=306). However, a strong
522 correlation was found between the total fluorescent intensity F_T and elevation (R^2=0.64,

523 N=306), suggesting that humic-like materials were predominant of the FDOM in the
524 saline waters and tended to decrease with increasing altitude. That interpretation would
525 be consistent with the moderate negative correlation between elevation and humification
526 index (HIX) (R^2=0.56, N=306), and the strong correlation between elevation and Fn(355)
527 (R^2=0.70, N=306), indicating that the concentration of humic-like substances and the
528 contribution of allochthonous sources of CDOM tended to decline in the high altitude
529 lakes due to the preferred degradation processes.

530 The linkages between fluorescent CDOM characteristics and elevation in the saline
531 lakes can be difficult to explain based solely on the data collected during the present
532 study. However, in light of the information presented in past studies, several
533 mechanisms can be invoked to explain the observed trends regarding lakes elevation
534 and fluorescence characteristics of CDOM in these lakes. Solar radiation is a key factor
535 for photo-induced degradation of DOM and organic contaminants in waters (Dobrovic´
536 et al., 2007; Mostofa et al., 2009). Previous studies have shown that increase in the
537 fluxes of UV radiation can substantially increase the quantity of reactive free radicals
538 such as HO• and H_2O_2 in waters (Qian et al., 2001; Yocis et al., 2000). The effect of
539 irradiance on the degradation processes and fluorescence properties of CDOM are
540 generally highest in surface waters, but tends to be less significant in regard to

deep-water DOM because of the lower sunlight irradiance in the deeper water layers (Laurion et al., 2000). Analysis of the relationships between lakes elevation and meteorological factors (100 stations), showed a moderate positive correlation with solar irradiance (R^2=0.41, N=100, p<0.01) and a weak positive correlation with duration of daylight (R^2=0.18, N=100, p<0.01) (Fig. S4). This result indicated that with increased lakes elevation, solar irradiance is a determining factor controlling the decrease in the humic-like fluorescent component of CDOM. Solar irradiation can trigger photo-induced degradation of CDOM and the release of small molecular weight CDOM moieties. The intensity of these processes and their impact on the concentration, absorption spectrum and molecular attributes of CDOM are expected to vary depending on lakes altitude. It demonstrated that the humic materials in CDOM undergo the photo-induced degradation in natural waters and would decrease significantly with increased elevation.

The relationships between FDOM and elevation can therefore be complex, and depend on several factors related to variable local conditions including, solar radiation, molecular nature of DOM, salinity and even global warming. Further investigations of these factors are needed to further elucidate the transformation of CDOM components, and the contribution of photo-induced reactions and microbial processes on these

559 transformations. These future studies would inform our understanding of photo-induced
560 and microbial-mediated alterations in CDOM absorption characteristics in inland waters,
561 and ultimately contribute to our ability to assess the significance of lacustrine
562 ecosystems to the global C cycle.
563

564 ## 5. Conclusions

565 Information about the optical properties and fluorescence characteristics of CDOM in
566 saline inland waters for large geographical regions is rare and generally incomplete. For
567 a better understanding of carbon cycling in inland lakes, a large-scale study was
568 conducted across five lake regions in China to explore the characteristics of CDOM
569 absorption and CDOM fluorescence. Compared to freshwater lakes, higher DOC
570 concentration, $a_{CDOM}(254)$ and $SUVA_{254}$ were measured in the saline inland lakes.
571 Analysis of CDOM fluorescence characteristics provided important insights regarding
572 the sources (allochthonous vs authochnous, natural vs anthropogenic), fates and
573 transformation of DOM in inland lakes. Specifically, the analysis showed that low
574 molecular CDOM fractions were relatively more abundant (hence, low humification
575 index of CDOM) in saline than in freshwater lakes. Since the saline lakes are largely
576 located in endorheic drainage basins and experience long periods of exposure to solar

577 radiation, these results were interpreted as the consequence of UV-induced
578 photochemical oxidation reactions in saline lakes whereby complex humic molecules
579 are decomposed into low molecular weight fulvic-like substances. Our results further
580 indicate that this photo-oxidation process is much stronger in high-altitude lakes. These
581 findings have important implications regarding our understanding of C dynamics in
582 inland lacustrine systems and the contribution of these ecosystems to the global C cycle.
583
584

585 **Acknowledgements**

586 The research was jointly supported by the National Natural Science Foundation of
587 China (41730104), the “hundred-talent program” from Chinese Academy of Sciences
588 granted to Dr. Kaishan Song, the Strategic Priority Research Program of the Chinese
589 Academy of Sciences（XDA19070501) and the National Natural Science Foundation of
590 China (41871234). The authors thank all staff and students for their persistent assistance
591 with both field sampling and laboratory analysis. We are grateful to the two anonymous
592 reviewers for their constructive comments and suggestions.
593
594

595 **References**

596 Adams, J. L., Tipping E., Feuchtmayr H., Carter H. T., and Keenan P. 2018. The contribution of
597 algae to freshwater dissolved organic matter: implications for UV spectroscopic
598 analysis. Inland Waters**:** 1-12.

599 Aullómaestro, M. E., Hunter P., Spyrakos E., Mercatoris P., Kovács A., Horváth H., Preston T.,
600 Présing M., Palenzuela J. T., and Tyler A. 2017. Spatio-seasonal variability of
601 chromophoric dissolved organic matter absorption and responses to photobleaching in a
602 large shallow temperate lake. Biogeosciences **14:** 1-41.

603 Bilal, M., Jaffrezic A., Dudal Y., Le G. C., Menasseri S., and Walter C. 2010. Discrimination of
604 farm waste contamination by fluorescence spectroscopy coupled with multivariate
605 analysis during a biodegradation study. J Agric Food Chem **58:** 3093-3100.

606 Blough, N. V., and Vecchio R. D. 2002. Chromophoric DOM in the Coastal Environment.
607 Elsevier Inc.

608 Brooks, M. L., Meyer J. S., and Mcknight D. M. 2007. Photooxidation of wetland and riverine
609 dissolved organic matter: altered copper complexation and organic composition.
610 Hydrobiologia **579:** 95-113.

611 Brooks, P. D., and Lemon M. M. 2015. Spatial variability in dissolved organic matter and
612 inorganic nitrogen concentrations in a semiarid stream, San Pedro River, Arizona.
613 Journal of Geophysical Research Biogeosciences **112:** 113-119.

614 Catalan, N., Marce, R., Kothawala, D.N., and Tranvik, L.J., 2016. Organic carbon
615 decomposition rates controlled by water retention time across inland waters. Nature
616 Geoscience 9: 501.

617 Chen, W., Westerhoff P., Leenheer J. A., and Booksh K. 2003. Fluorescence excitation-emission
618 matrix regional integration to quantify spectra for dissolved organic matter.
619 Environmental Science & Technology **37:** 5701-5710.

620 Coble, P. G. 1996. Characterization of marine and terrestrial DOM in seawater using
621 excitation-emission matrix spectroscopy. Marine Chemistry **51:** 325-346.

622 Coble, P. G. 2007. Marine optical biogeochemistry: the chemistry of ocean color. Cheminform
623 **38:** 402-418.

624 Curtis, P. J., and Adams H. E. 1995. Dissolved Organic Matter Quantity and Quality from

Freshwater and Saltwater Lakes in East-Central Alberta. Biogeochemistry **30:** 59-76.

Dobrović, S., Juretić H., and Ružinski N. 2007. Photodegradation of Natural Organic Matter in Water with UV Irradiation at 185 and 254 nm: Importance of Hydrodynamic Conditions on the Decomposition Rate. Separation Science & Technology **42:** 1421-1432.

Effler, S. W., Perkins M. G., Peng F., Strait C., Weidemann A. D., and Auer M. T. 2010. Light-absorbing components in Lake Superior. Journal of Great Lakes Research **36:** 656-665.

Fichot, C. G., and Miller W. L. 2010. An approach to quantify depth-resolved marine photochemical fluxes using remote sensing: Application to carbon monoxide (CO) photoproduction. Remote Sensing of Environment **114:** 1363-1377.

Fichot, C. G., and Ronald B. 2012. The spectral slope coefficient of chromophoric dissolved organic matter (S275–295) as a tracer of terrigenous dissolved organic carbon in river-influenced margins. Limnology & Oceanography **57:** 1453-1466.

Gonnelli, M. 2013. Chromophoric dissolved organic matter and microbial enzymatic activity. a biophysical approach to understand the marine carbon cycle. Biophysical Chemistry, 182(1), 79-85.

Helms, J. R., Stubbins A., Ritchie J. D., Minor E. C., Kieber D. J., and Mopper K. 2008. Absorption spectral slopes and slope ratios as indicators of molecular weight, source, and photobleaching of chromophoric dissolved organic matter. Limnology & Oceanography **53:** 955-969.

Henderson, J. N., Osborn M. F., Koon N., Gepshtein R., Huppert D., and Remington S. J. 2009. Excited State Proton Transfer in the Red Fluorescent Protein mKeima. Journal of the American Chemical Society **131:** 13212.

Jansson, M., Bergström A. K., Blomqvist P., and Drakare S. 2000. Allochthonous organic carbon and phytoplankton/bacterioplankton production relationships in lakes. Ecology **81:** 3250-3255.

Jian, S., Liang G., Li Q., Zhao Y., Gao M., She Z., and Jin C. 2016. Three-dimensional fluorescence excitation–emission matrix (EEM) spectroscopy with regional integration analysis for assessing waste sludge hydrolysis at different pretreated temperatures. Environmental Science & Pollution Research **23:** 24061-24067.

Kellerman, A. M., Kothawala, D. N., Dittmar, T., and Tranvik, L. J. 2015. Persistence of

dissolved organic matter in lakes related to its molecular characteristics. Nature Geoscience **8:** 454-457.

Kothawala, D. N., Stedmon C. A., Müller R. A., Weyhenmeyer G. A., Köhler S. J., and Tranvik L. J. 2014. Controls of dissolved organic matter quality: evidence from a large‐scale boreal lake survey. Global Change Biology **20:** 1101-1114.

Kramer, J. B., Silvio Canonica A., Hoigné J., and Kaschig J. 1996. Degradation of Fluorescent Whitening Agents in Sunlit Natural Waters. Environmental Science & Technology **30:** 2227-2234.

Lawaetz, A. J., and Stedmon C. A. 2009. Fluorescence Intensity Calibration Using the Raman Scatter Peak of Water. Applied Spectroscopy **63:** 936-940.

Ma, R. H., Wang S. M., Li A. N., Wu J. L., Yang G. S., Duan H. T., Jiang J. H., Feng X. Z., Kong F. X., and Xue B. 2011. China's lakes at present:Number,area and spatial distribution. Science China Earth Sciences **54:** 283-289.

Madsen- sterbye, M., Kragh T., Pedersen O., and Sand-Jensen K. 2018. Coupled UV-exposure and microbial decomposition improves measures of organic matter degradation and light models in humic lake. Ecological Engineering **118:** 191-200.

Mcknight, D. M., Boyer E. W., Westerhoff P. K., Doran P. T., Kulbe T., and Andersen D. T. 2001. Spectrofluorometric Characterization of Dissolved Organic Matter for Indication of Precursor Organic Material and Aromaticity. Limnology & Oceanography **46:** 38-48.

Minakata, D., Li K., Westerhoff P., and Crittenden J. 2009. Development of a group contribution method to predict aqueous phase hydroxyl radical (HO*) reaction rate constants. Environmental Science & Technology **43:** 6220.

Minero, C., Chiron S., Falletti G., Maurino V., Pelizzetti E., Ajassa R., Carlotti M. E., and Vione D. 2007. Photochemincal processes involving nitrite in surface water samples. Aquatic Sciences **69:** 71-85.

Moran, M. A., Sheldon W. M., and Jr. 2000. Carbon loss and optical property changes during long-term photochemical and biological degradation of estuarine dissolved organic matter. Limnology & Oceanography **45:** 1254-1264.

Mostofa, K. M. G. 2009. Dissolved organic matter in the aquatic environments. Natural Organic Matter & Its Significance in the Environment.

Nieto-Cid, M., lvarez-Salgado X. A., and Pérez F. F. 2006. Microbial and photochemical

reactivity of fluorescent dissolved organic matter in a coastal upwelling system. Limnology & Oceanography **51:** 1391-1400.

Oki T., Kanae S. 2006. Global hydrological cycles and world water resources. Science 313: 1068-1072.

Osburn, C. L., O'sullivan D. W., and Boyd T. J. 2009. Increases in the longwave photobleaching of chromophoric dissolved organic matter in coastal waters. Limnology & Oceanography **54:** 145–159.

Para, J., Coble P. G., Charrière B., Tedetti M., Fontana C., and Sempéré R. 2010. Fluorescence and absorption properties of chromophoric dissolved organic matter (CDOM) in coastal surface waters of the northwestern Mediterranean Sea, influence of the Rhône River. Biogeosciences **7:** 4083-4103.

Qian, J., Mopper K., and Kieber D. J. 2001. Photochemical production of the hydroxyl radical in Antarctic waters. Deep Sea Research Part I Oceanographic Research Papers **48:** 741-759.

Rochelle-Newall, E. J., and Fisher T. R. 2002. Production of chromophoric dissolved organic matter fluorescence in marine and estuarine environments: an investigation into the role of phytoplankton. Marine Chemistry **77:** 7-21.

Shank, G. C., Lee R., Vähätalo A., Zepp R. G., and Bartels E. 2010. Production of chromophoric dissolved organic matter from mangrove leaf litter and floating Sargassum colonies. Marine Chemistry **119:** 172-181.

Singh, S., D'sa E. J., and Swenson E. M. 2010. Chromophoric dissolved organic matter (CDOM) variability in Barataria Basin using excitation-emission matrix (EEM) fluorescence and parallel factor analysis (PARAFAC). Science of the Total Environment **408:** 3211-3222.

Song, K., Wen Z., Xu Y., Yang H., Lyu L., Zhao Y., Fang C., Shang Y., and Du J. 2018. Dissolved carbon in a large variety of lakes across five limnetic regions in China. Journal of Hydrology **563:**143-154.

Song, K. S., Zang S. Y., Zhao Y., Li L., Du J., Zhang N. N., Wang X. D., Shao T. T., Guan Y., and Liu L. 2013. Spatiotemporal characterization of dissolved carbon for inland waters in semi-humid/semi-arid region, China. Hydrology & Earth System Sciences, **10:** 4269-4281.

Spencer, R. G. M., Butler K. D., and Aiken G. R. 2015. Dissolved organic carbon and

chromophoric dissolved organic matter properties of rivers in the USA. Journal of Geophysical Research Biogeosciences **117:** 3001.

Stedmon, C. A., and Bro R. 2008. Characterizing dissolved organic matter fluorescence with parallel factor analysis: a tutorial. Limnology & Oceanography Methods **6:** 572-579.

Stedmon, C. A., Markager S., and Bro R. 2003. Tracing dissolved organic matter in aquatic environments using a new approach to fluorescence spectroscopy. Marine Chemistry **82:** 239-254.

Swietlik, J. and Sikorska, E. 2004. Application of fluorescence spectroscopy in the studies of natural organic matter fractions reactivity with chlorine dioxide and ozone. Water Research, 38(17), 3791-3799.

Sun, L., and Mopper K. 2016. Studies on Hydroxyl Radical Formation and Correlated Photoflocculation Process Using Degraded Wood Leachate as a CDOM Source. Frontiers in Marine Science **2**.

Tranvik, L. J., Downing J. A., Cotner J. B., Loiselle S. A., Striegl R. G., Ballatore T. J., Dillon P., Finlay K., Fortino K., and Knoll L. B. 2009. Lakes and reservoirs as regulators of carbon cycling and climate. Limnology & Oceanography **54:** 2298-2314.

Vione, D., Falletti G., Maurino V., Minero C., Pelizzetti E., Malandrino M., Ajassa R., Olariu R. I., and Arsene C. 2006. Sources and sinks of hydroxyl radicals upon irradiation of natural water samples. Environmental Science & Technology **40:** 3775-3781.

Vione, D., Khanra S., Das R., Minero C., Maurino V., Brigante M., and Mailhot G. 2010. Effect of dissolved organic compounds on the photodegradation of the herbicide MCPA in aqueous solution. Water research **44:** 6053-6062.

Webster, K. E., Soranno P. A., Cheruvelil K. S., Bremigan M. T., Downing J. A., Vaux P. D., Asplund T. R., Bacon L. C., and Connor J. 2008. An Empirical Evaluation of the Nutrient-Color Paradigm for Lakes. Limnology & Oceanography **53:** 1137-1148.

Weishaar, J. L., Aiken G. R., Bergamaschi B. A., Fram M. S., Fujii R., and Mopper K. 2003. Evaluation of specific ultraviolet absorbance as an indicator of the chemical composition and reactivity of dissolved organic carbon. Environmental Science & Technology **37:** 4702-4708.

Wen, Z., Song K., Shang Y., Zhao Y., Fang C., and Lyu L. 2018. Differences in the distribution and optical properties of DOM between fresh and saline lakes in a semi-arid area of

Northern China. Aquatic Sciences **80:** 22.

Wen, Z. D., Song K. S., Zhao Y., Du J., and Ma J. H. 2015. Influence of environmental factors on spectral characteristic of chromophoric dissolved organic matter (CDOM) in Inner Mongolia Plateau, China. Hydrology & Earth System Sciences, **12:** 5895-5929.

Yocis, B. H., Kieber D. J., and Mopper K. 2000. Photochemical production of hydrogen peroxide in Antarctic Waters. Deep Sea Research Part I Oceanographic Research Papers **47:** 1077-1099.

Zhang, Y., Zhou, Y., Shi, K., Qin, B., Yao, X., & Zhang, Y. 2018. Optical properties and composition changes in chromophoric dissolved organic matter along trophic gradients: implications for monitoring and assessing lake eutrophication. Water Research, 131, 255.

Zhang, Y., Gao G., Shi K., Niu C., Zhou Y., Qin B., and Liu X. 2014. Absorption and fluorescence characteristics of rainwater CDOM and contribution to Lake Taihu, China. Atmospheric Environment **98:** 483-491.

Zhang, Y., Van Dijk M. A., Liu M., Zhu G., and Qin B. 2009. The contribution of phytoplankton degradation to chromophoric dissolved organic matter (CDOM) in eutrophic shallow lakes: Field and experimental evidence. Water research **43:** 4685-4697.

Zhang, Y., Yin Y., Liu X., Shi Z., Feng L., Liu M., Zhu G., Gong Z., and Qin B. 2011. Spatial-seasonal dynamics of chromophoric dissolved organic matter in Lake Taihu, a large eutrophic, shallow lake in China. Organic Geochemistry **42:** 510-519.

Zhao, Y., Song K., Shang Y., Shao T., Wen Z., and Lv L. 2017. Characterization of CDOM of river waters in China using fluorescence excitation-emission matrix and regional integration techniques. Journal of Geophysical Research-Biogeosciences **122:** 1940-1953.

Zhao, Y., Song K., Wen Z., Li L., Zang S., Shao T., Li S., and Du J. 2016. Seasonal characterization of CDOM for lakes in semiarid regions of Northeast China using excitation-emission matrix fluorescence and parallel factor analysis (EEM-PARAFAC). Biogeosciences **13:** 1635-1645.

Zhou, Y., Zhang, Y., Jeppesen, E., Murphy, K. R., Shi, K., & Liu, M., et al. 2016. Inflow rate-driven changes in the composition and dynamics of chromophoric dissolved organic matter in a large drinking water lake. Water Research, 100, 211-221.

Tables

Table 1 The Excitation and Emission wavelength ranges of the five integrated regions identified by Fluorescence Regional Integration (FRI) *

FRI Region	Excitation (nm)	Emission (nm)	Description and Source
F_1	200-250	250-330	Tyrosine-like protein
F_2	200-250	330-350	Tryptophan-like protein
F_3	200-250	350-500	Fulvic acid-like
F_4	250-280	250-380	Microbial-like
F_5	280-400	380-500	Humic-like

*Five regions identified by FRI method according to Chen et al. (2003).

Table 2 The water chemical parameters of various lake regions

Region	DOC (mg/L)	EC （μs/cm）	TN (mg/L)	TP (mg/L)	Chl-a (mg/L)	TSM (mg/L)
NLR	27.22	3855.21	5.54	1.28	24.10	127.00
MXR	25.78	9388.91	3.23	0.17	6.99	24.88
TQR	34.96	9671.30	3.82	0.49	1.94	29.64
ELR	5.92	345.32	0.98	0.02	55.21	13.33
YGR	5.25	388.12	0.90	0.05	24.41	41.99
All saline	27.40	12722.98	3.55	0.40	7.01	42.97
All Fresh	6.68	970.75	2.38	0.13	47.99	19.91

Table 3 The PCA component 1 and 2 as the dependent variables expressed with FRI fluorescent components as independent variables

Types	Equations
Saline waters	Component 1=$0.417F_1+0.501F_2+0.484F_3+0.446F_4+0.377F_5$
	Component 2=$-0.564F_1-0.014F_2+0.373F_3-0.390F_4+0.625F_5$
Fresh waters	Component 1=$0.457F_1+0.473F_2+0.430F_3+0.468F_4+0.404F_5$
	Component 2=$-0.427F_1-0.266F_2+0.506F_3-0.319F_4+0.624F_5$

Figures

Fig. 1 The distribution of sampled saline and freshwater lakes in different lake regions with respecting to elevation across China.

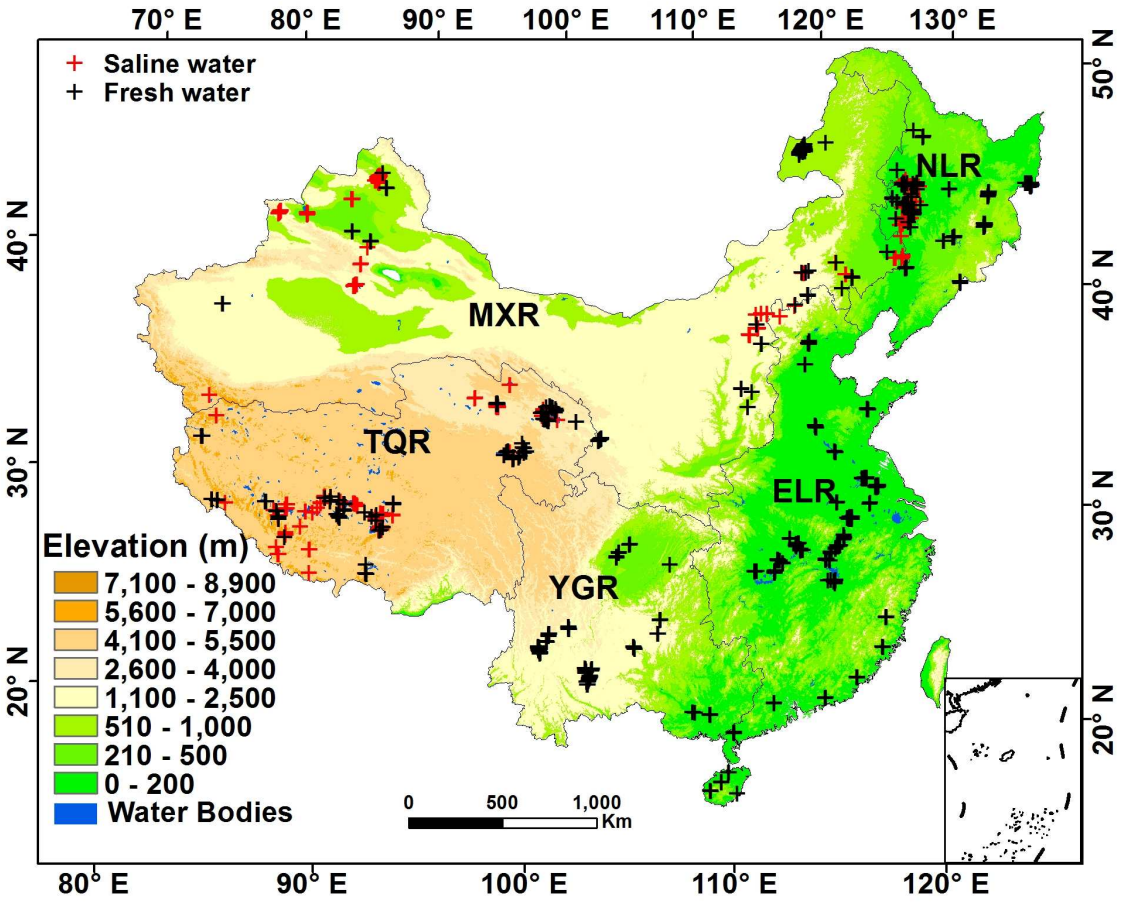

Fig. 2 (a) the concentration variations of dissolved organic carbon (DOC), and (b) the variation of $a_{CDOM}(254)$ and comparison for saline (S) and fresh waters (F) in five lake regions across China.

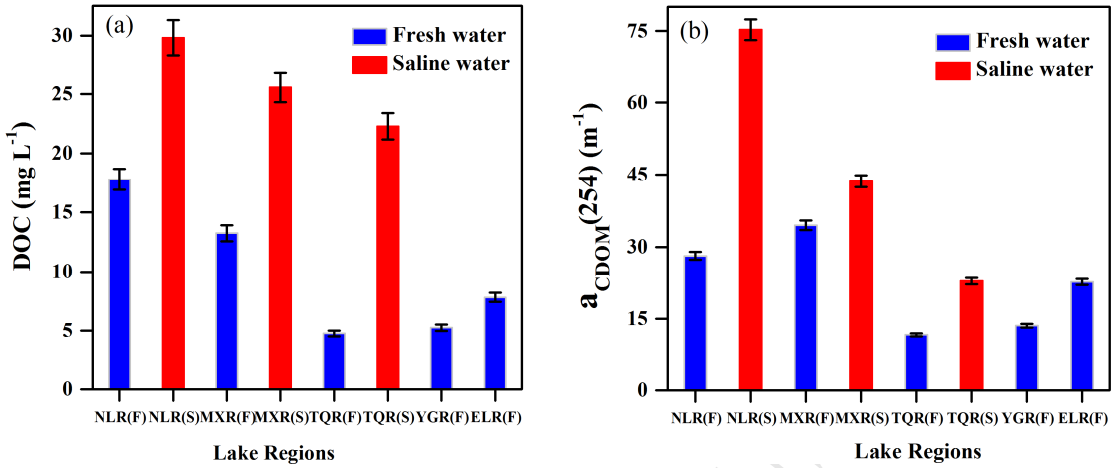

Fig. 3(a) The variation and comparison of CDOM absorption spectral slope ($S_{275\text{-}295}$), and (b) $SUVA_{254}$ values for saline (S) and freshwater (F) lakes across five lake regions of China. The line and circle within each box represent the median and mean, respectively. The horizontal edges of each box denote the 25th and 75th percentiles, the whiskers denote the 10th and 90th percentiles, and × represent outliers.

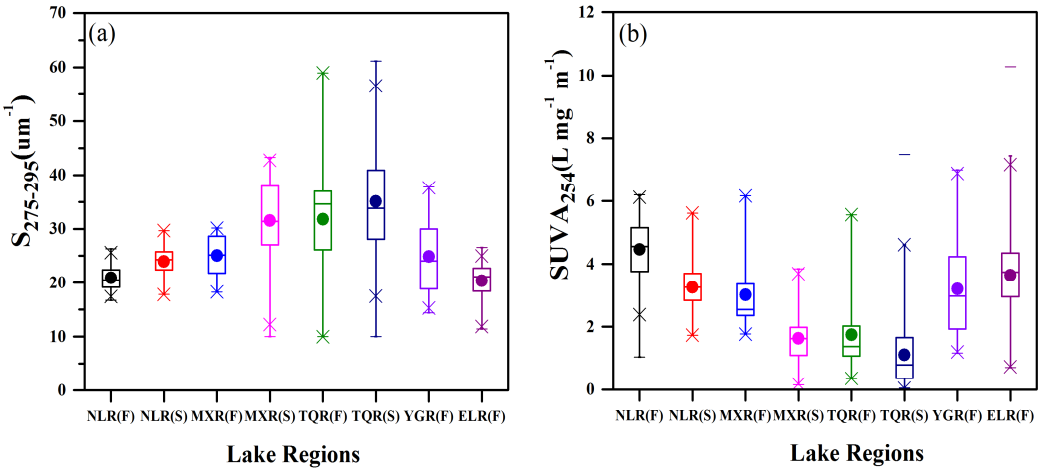

Fig. 4 The EEM fluorescence spectra and FRI distribution of Lake Selin Co from the TQR, Lake Aibi from the MXR and Lake Khanka from the NLR.

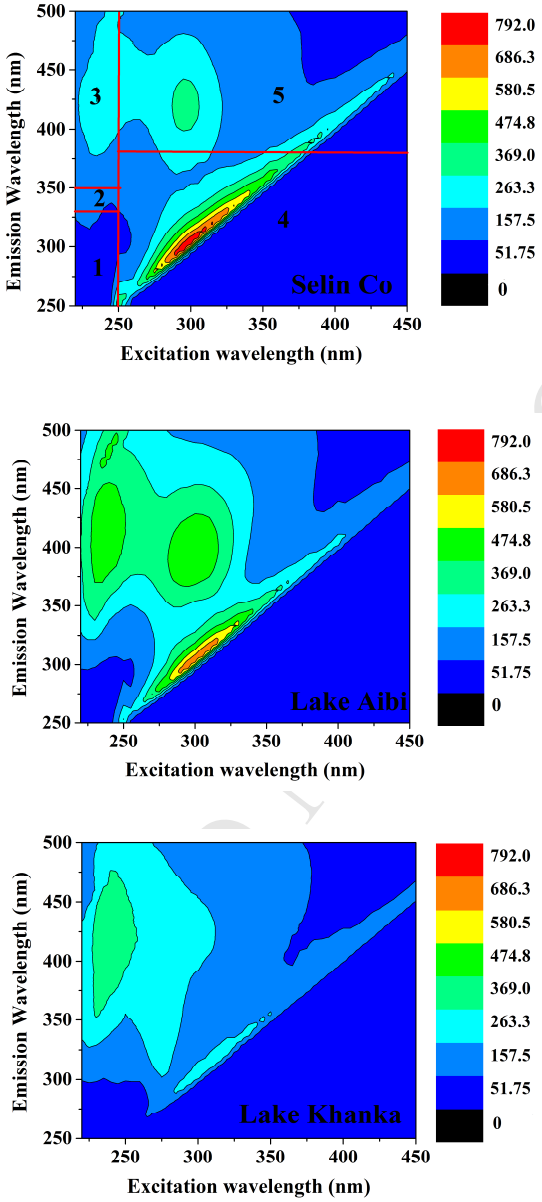

Fig.5 The comparison of total fluorescent intensity of saline (S) and fresh water (F) lakes in different lake regions across China.

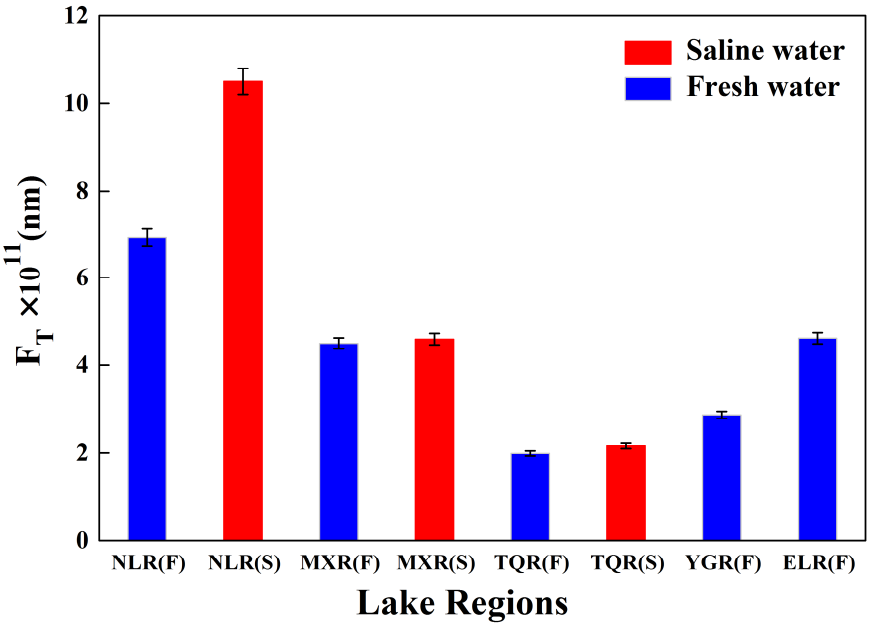

Fig. 6 The comparison of individual fluorescent intensities of saline (S) and fresh waters (F) in different lake regions. F1 represents tyrosine-like protein, F2 represents tryptophan-like protein, F3 represents fulvic acid-like organics, F4 represents soluble microbial by-product-like materials, and F5 represents humic acid-like organics

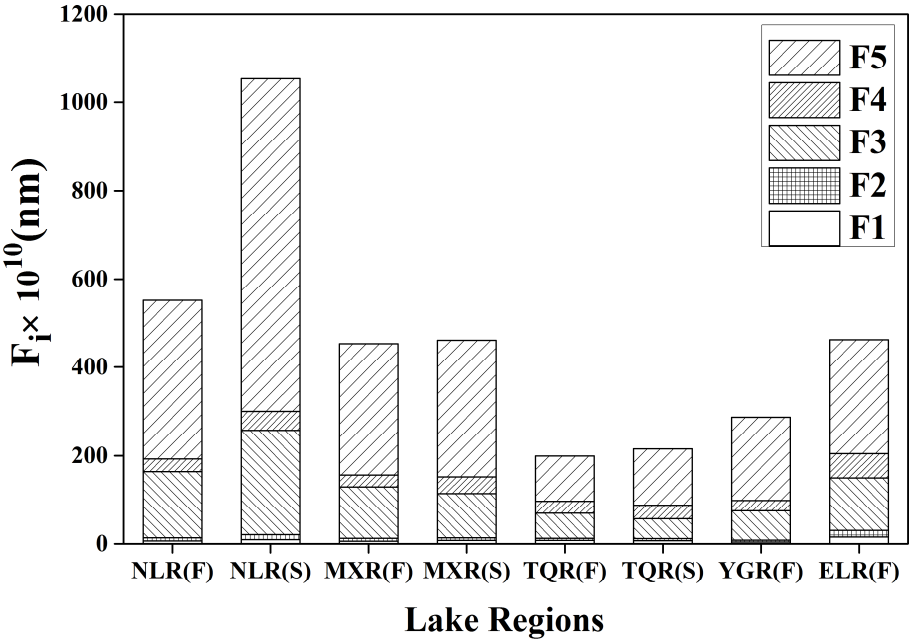

Fig. 7 The proportions of individual fluorescent intensities of saline (S) and fresh waters (F) in different lake regions. P_1 represents the percentages of EEM-FRI extracted FDOM related to tyrosine-like protein. P_2 represents the percentages of EEM-FRI extracted FDOM related to tryptophan-like protein. P_3 represents the percentages of EEM-FRI extracted FDOM related to fulvic acid-like organics. P_4 represents the percentages of EEM-FRI extracted FDOM related to soluble microbial by-product-like materials. P_5 represents the percentages of EEM-FRI extracted FDOM related to humic acid-like organics.

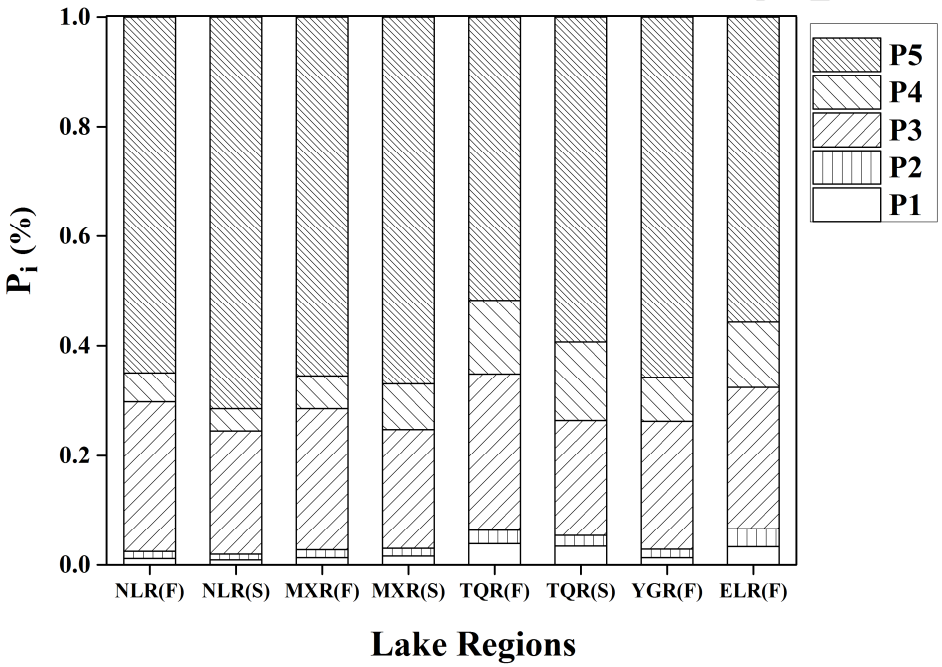

Fig. 8 The principal component analysis (PCA) results of FRI-based EEMs (a) PCA components and (b) PCA factor scores for saline waters; (c) PCA components and (d) PCA factor scores for freshwaters.

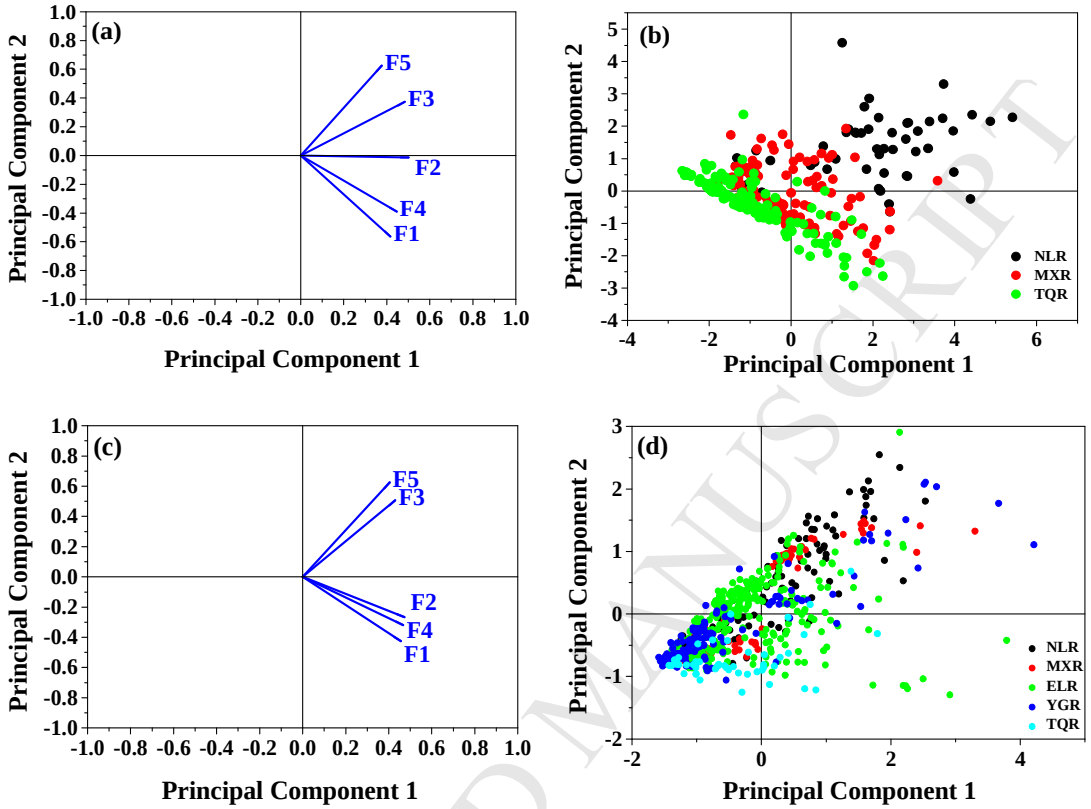

Fig. 9 The correlation between $a_{CDOM}(254)$ and DOC concentration for various lake regions in China. (a). TQR (The high saline waters are with the mean EC of 25000 us/cm, the low saline water are with the mean EC of 9500 us/cm); (b). ELR; (c). YGR; (d). NLR; (e). MXR.

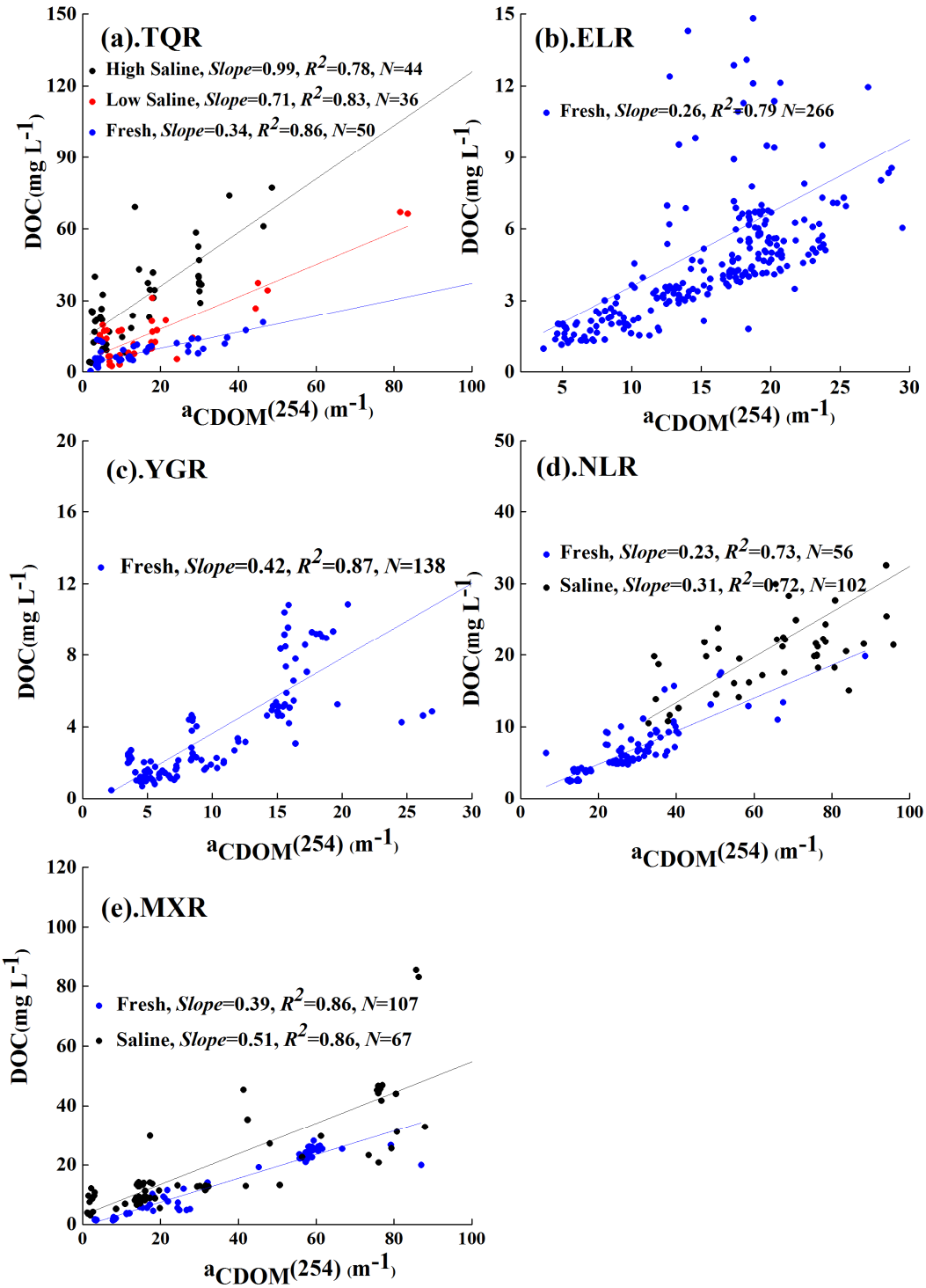

Fig.10 The correlations between a_{CDOM} (254) and FRI-EEMs characteristics, (a). cumulative volume F_1 and F_4 by EEM-FRI for water samples in saline lakes, (b) $a_{CDOM}(254)$ and Humic-like Fluorescence (Fn355), (c) $a_{CDOM}(254)$ and humification index, (d) cumulative volume F_2 and F_3 by EEM-FRI for water samples in saline lakes, (e) $a_{CDOM}(254)$ and cumulative volume F_3+F_5 by EEM-FRI for water samples in saline lakes, (f) cumulative volume F_3 and F_5 by EEM-FRI for water samples in saline lakes.

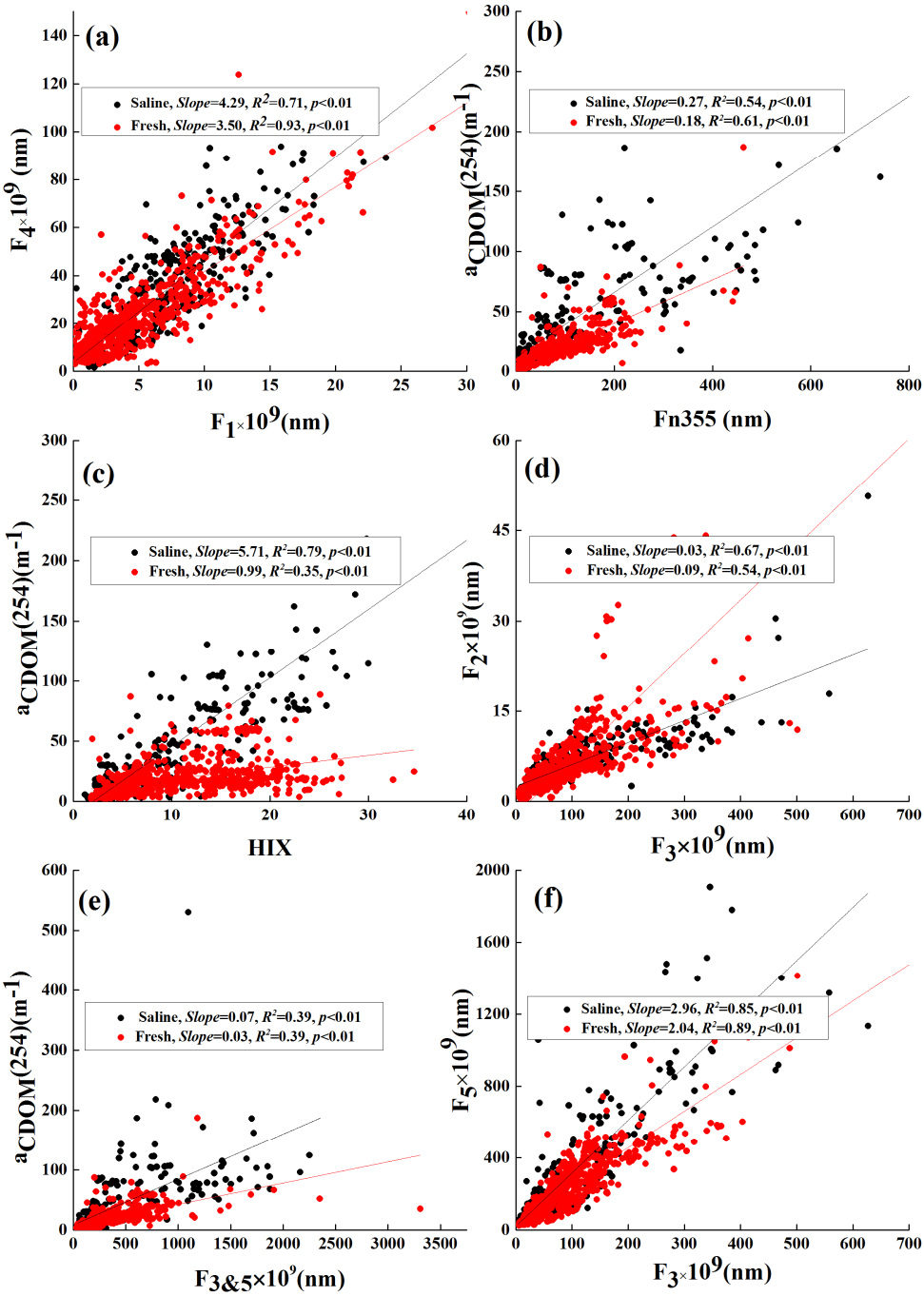

Fig. 11 The correlation between elevation and CDOM absorption and FRI-EEM extracted indices for saline waters, (a) $a_{CDOM}(254)$ versus elevation, (b) F_5 versus elevation, (c) F_n355 versus elevation, (d) F_T versus elevation, (e) HIX and elevation, and (f) $SUVA_{254}$ versus elevation.

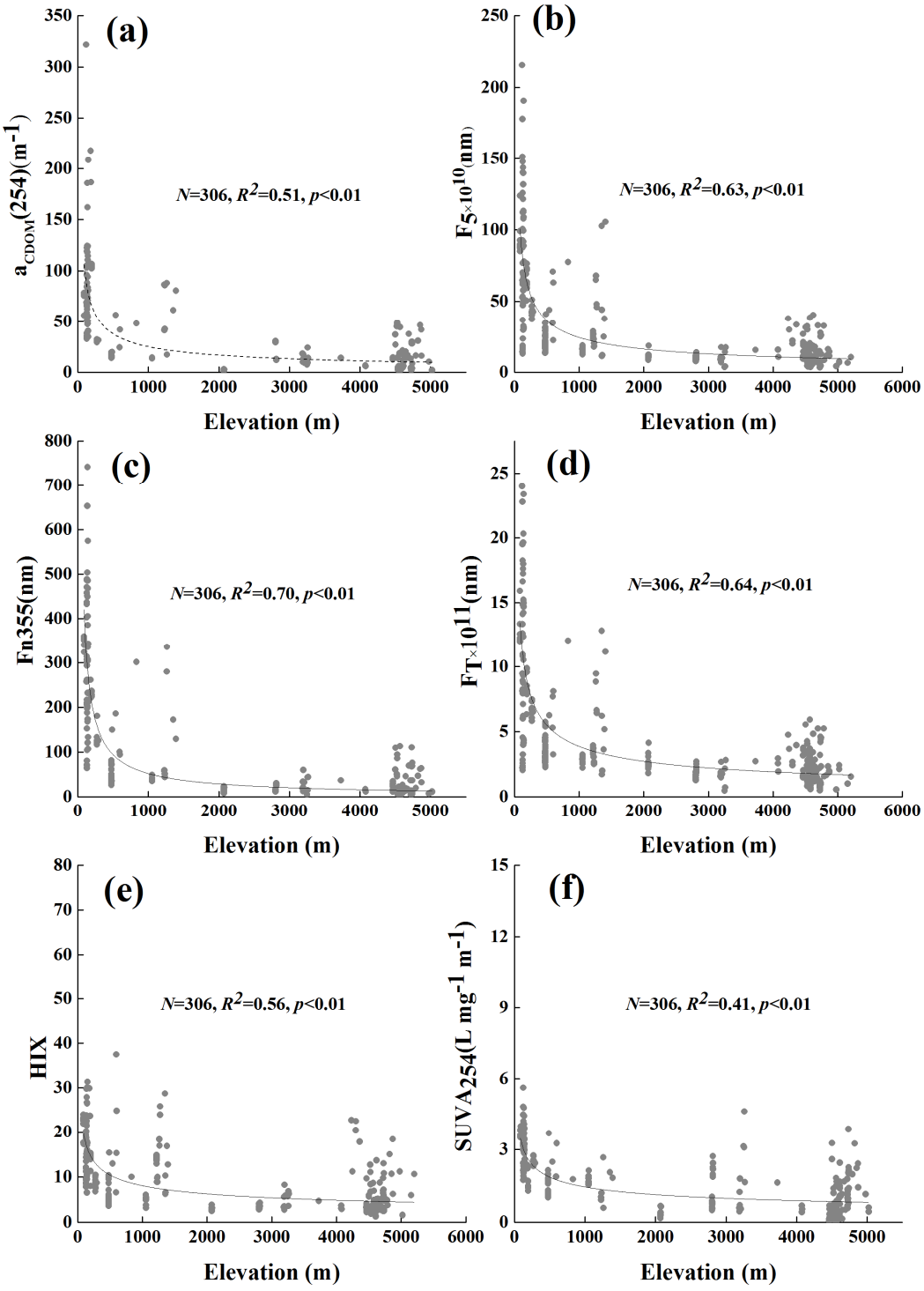

Highlights

1. The 936 lake samples in China were examined to explore CDOM optical properties

2. FRI was used to characterize CDOM sources of saline waters and fresh waters

3. The relationships between CDOM absorption and FDOM components were analyzed

4. Close relations of elevation and saline waters FDOM components were identified

Declaration of interests

☒ The authors declare that they have no known competing financial interests or personal relationships that could have appeared to influence the work reported in this paper.

☐The authors declare the following financial interests/personal relationships which may be considered as potential competing interests: